The 2nd Spitzer Conference: Infrared Diagnostics of Galaxy Evolution
ASP Conference Series, Vol. 381, ©*2008*
Ranga-Ram Chary, Harry I. Teplitz, Kartik Sheth, eds.

MIPS Class Coaddition of SWIRE High-Redshift Galaxies

David L. Shupe

Spitzer Science Center, MS 314-6, Caltech, Pasadena, CA 91125, USA

Carol J. Lonsdale, Mari Polletta

Center for Astrophysics and Space Sciences, University of California at San Diego, La Jolla, CA 92093, USA

Guilaine Lagache

Institut d'Astrophysique Spatiale, Université Paris-Sud, bât 121, F-91405 Orsay Cedex, France

Abstract. The SWIRE survey encompasses the largest volume of the Spitzer extragalactic surveys, providing the best sensitivity for the detection of significant numbers of rare objects, including the most massive ULIRGs, and obscured AGN. These objects are detected and classified using Spitzer IRAC and MIPS-24 data, but are too faint to be detected individually in the 70 μm and 160 μm bands. We have applied a class coaddition technique to investigate far-infrared spectral energy distributions of these sources by redshift and spectral shape. The variation of far-IR-to-mid-IR colors of the ULIRGs with redshift generally tracks the predictions of template galaxies, and favors the lower-luminosity templates.

1. Class Coaddition Method

The coadding technique used in this work follows the method used by Dole et al. (2006) to measure the contribution of 24 μm sources to the extragalactic background at 70 μm and 160 μm. We begin with a list of sources detected at shorter wavelengths (usually including 24 μm), but without detections in the longer MIPS bands. At each of the positions of the sources, we extract a subimage out of the full-field SWIRE mosaics. The subimages are placed into a stack twice, once with their original orientation, and again with a 90 degree rotation, to ameliorate instrumental effects. Then a 10% trimmed mean and the median are computed.

An uncertainty or confidence interval estimate is produced using a bootstrap technique. A set of subimages is drawn from the stack randomly without replacement, to make a new sample of the same size as that being coadded. The trimmed mean and the median are computed for this set, and the resulting photometry is recorded. The resampling is repeated typically 1000 times to fill out the distribution. The standard deviation of the values yields an uncertainty estimate.

The stacking code is written entirely in Python and makes extensive use of the PyFITS and numarray packages developed by STScI.

2. Application to ULIRGs in the SWIRE Survey

The sample of ULIRGs used in this study is described by Lonsdale (this proceedings). The SWIRE optical, IRAC, and MIPS-24 data have been used to select ULIRG candidates which show clear evidence in the IRAC bands for spectral energy distributions which peak near 1.6 μm rest-frame, due to the H- opacity minimum in the atmospheres of evolved stars (Sawicki et al. 2002). Selecting sources with peaks in IRAC Ch2 (4.5 μm) or IRAC Ch3 (5.8 μm) yields a sample of sources with photometric redshifts ranging from 1.2 to greater than 3. The selection discriminates against both low-z sources and against AGN. The sample has a minimum 24 μm flux of 0.4 mJy, yielding hundreds of ULIRG candidates in each SWIRE field.

Only a handful of these sources are detected in the MIPS 70 μm and 160 μm bands, however. The large sample size is well-suited to the class coaddition technique, since the positions of the sources are well-determined from the short-wavelength data. We have coadded subsamples divided by various criteria including photometric redshift, absolute 3.6 μm magnitude, and infrared luminosity (for each of three template types: NGC 6090(SB), Arp 220, and I22491).

The primary classification of interest is by photometric redshift range. We subdivided the "bump 2" (4.5 μm-peaking) sources into $1 < z < 1.6$ and $1.6 < z < 2.2$ ranges. The "bump 3" (5.8 μm-peaking) sources were subdivided into these photo-z ranges: 1.5-2.0, 2.0-2.3, 2.3-2.5, and 2.5-3.0. The resulting average colors from the coaddition technique are shown in Figure 1. For both colors, the variation with redshift follows template predictions in a relative sense, and the F(160 μm)/F(24 μm) values follow closely the NGC 6090(SB) template. The F(70 μm)/F(24 μm) values fall below all of the templates. More sources are detected in the 160 μm band than at 70 μm, and the individual detections follow the more extreme templates. The class coaddition results favor lower luminosities in the mean.

The interpretation of these colors is complicated by spectral features affecting the 24 μm band. Figure 2 shows normalized rest-frame templates for two of our redshift classes, with optical and IR photometry, and the coaddition results for each class.

3. Application to Obscured AGN

The class coadding technique was applied to the sample of obscured AGN of Polletta et al. (2006) in the SWIRE Lockman Hole field. The sample includes 87 sources with Chandra detections, classified into four categories based on the shorter-wavelength data: *Class I:* Very red IR SEDs with convex shapes, fit by a "Torus" template; *Class II:* Power-law-like optical-IR SEDs; *Class III:* Reddened QSO template; *Class IV:* AGN and star-formation components; *Class V:* Optical colors redder than IR colors; *Class VI:* Fainter galaxies with very red F(4.5 μm)/F(3.6 μm). Figure 3 shows a few examples from each class. The dotted line is the color derived from a class coadd of the each class. These example SEDs show the differences among the classes. The coaddition results generally indicate that the AGN have warm far-IR colors, although the small sample size leads to upper limits in some cases.

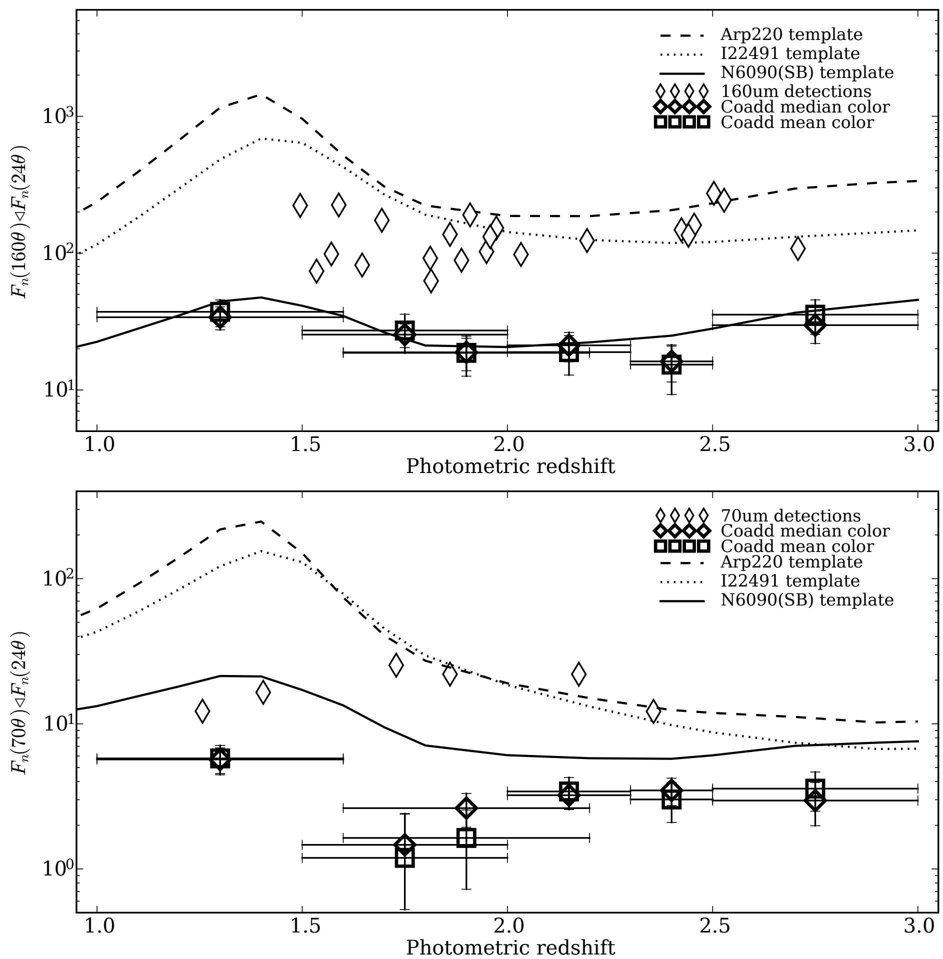

Figure 1. Variation with redshift of 160/24 (top) and 70/24 (bottom) colors. The thin diamonds show the colors for sources detected individually in the SWIRE data. The thick diamonds and squares indicate the colors determined from the class coadds. The x-errorbars indicate the z-ranges, and the y-errorbars are derived from the standard deviation of the bootstrap resamplings. The predicted colors for three templates are traced by the lines. The colors on the whole favor the NGC 6090 template and lower IR luminosities for these sources.

Acknowledgments. We are grateful to Hervé Dole for advice on estimating uncertainties using bootstrap resampling.

References

Dole, H., Lagache, G., Puget, J.-L., Caputi, K., Fernandez-Conde, N., Le Floc'h, E., Papovich, C., Perez-Gonzalez, P.G., Rieke, G.H., & Blaylock, M. 2006, A&A, in press (astro-ph/0603208).

Polletta, M., Wilkes, B.J., Siana, B., Lonsdale, C.J., Kilgard, R., Smith, H.E., Kim, D.-W., Owen, F., Efstathiou, A., Jarrett, T., Stacey, G., Franceschini, A., Rowan-

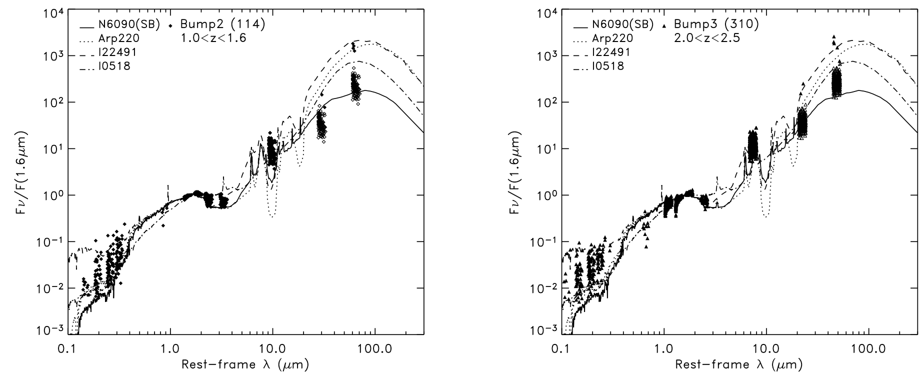

Figure 2. SEDs for different templates for some of the redshift classes. The templates are shown for rest-wavelength, and have been normalized at a rest wavelength of 1.6 μm. The optical, IRAC, and MIPS 24 photometry are plotted for each source after blue-shifting and normalization. The mean coadd color has been used to generate observed 70 μm and 160 μm photometry for each source undetected in those bands, which is why those point clouds have mostly the same distribution as the observed 24 μm points. The number of sources in each class is shown in parentheses.

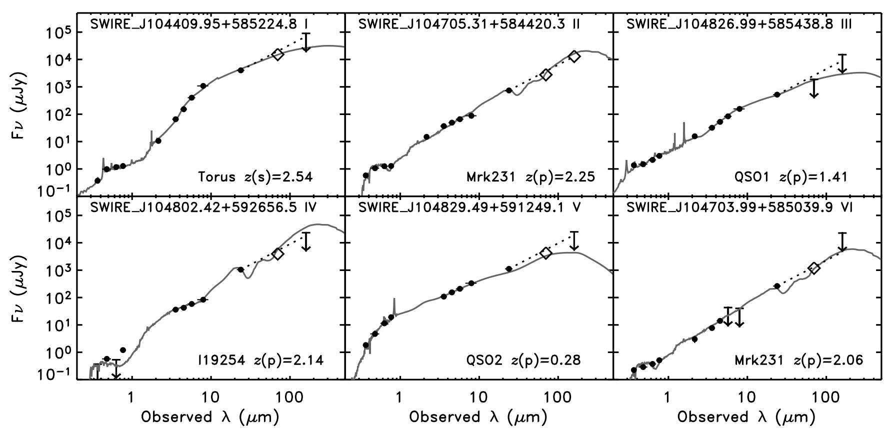

Figure 3. Example SEDs from the Lockman Hole obscured AGN sample described in (Polletta et al. 2006). The best-fitting templates for each of four classes is redshifted and normalized to the shorter-wavelength IRAC and MIPS-24 data. The dashed line indicates the average far-IR colors for the entire sample of 87 sources. The open diamonds are based on the 70/24 and 160/24 colors for individual class coadds.

Robinson, M., Babbedge, T.S.R., Berta, S., Fang, F., Farrah, D., Gonzalez-Solares, E., Morrison, G., Surace, J.A., & Shupe, D.L. 2006, ApJ, in press (astro-ph/0602228).
Sawicki, M. 2002, AJ, 124, 3050.